Supporting Material

High Resolution Conformation and Backbone Dynamics of a Soluble Aggregate of Apomyoglobin$_{1-119}$

Senapathy Rajagopalan[†], Neşe Kurt and Silvia Cavagnero*

Department of Chemistry, University of Wisconsin-Madison, 1101 University Avenue, Madison, Wisconsin 53706, USA.

[*] Corresponding author.

[†] Current address: The Methodist Hospital Research Institute, Diabetes Research, 6565 Fannin St, F8-060, Houston, TX, 77030 and UTMD Anderson Cancer Center, 1515 Holcombe Blvd., Unit 1000, Houston, TX, 77030.

Running Title: NMR Study of ApoMb$_{1-119}$ Soluble Aggregate

Keywords: protein backbone dynamics; misfolding; NMR; truncated globin; residual helicity; chaperone.

SUPPLEMENTARY MATERIALS & METHODS

NMR Chaperone Binding Titration. Chaperone binding titrations were carried out upon addition of increasing amounts of unlabeled apoMb$_{119}$ (from a concentrated stock solution at pH 2.5) to 90 μM ^{15}N-labeled DnaK-β in 10mM sodium acetate and 5% D_2O, at pH 6.0. The pH was adjusted to 6.0 after each addition of apoMb$_{119}$. The addition of substrate led to an increase in apoMb$_{119}$ concentration by 50 μM after each titration step, resulting in a final apoMb$_{119}$ concentration of 150 μM. Unfortunately, it was not possible to reach higher apoMb$_{119}$: ^{15}N-DnaK-β ratios in the course of this titration, due to the limited solubility of both species. Higher ratios at overall much lower concentrations of binding partners are in principle feasible but would impair NMR detection.

Backbone NMR Resonance Assignments. HN and N backbone resonances of apoMb$_{119}$ were identified upon comparison of the assigned HN and N resonances of apoMb$_{119}$ at pH 2.5 (1) to the endpoint of pH titrations on ^{15}N-apoMb$_{119}$. The pH titrations were carried out by collecting a series of ^{1}H-^{15}NHSQC spectra at pH 6.0 and progressively lower values, down to pH 2.5. HSQC time-domain data were zero-filled twice and apodized with an unshifted Gaussian in both dimensions. C^{α} chemical shifts of apoMb$_{119}$ were obtained by extending the ^{1}H and ^{15}N assignments to the corresponding C^{α} resonances via three-dimensional HNCA (2) experiments at pH 6.0 (68(t1), 37(t2), 1024(t3) complex points). HNCA time-domain data were linearly predicted (32points) in the ^{15}N dimension and zero-filled twice in all dimensions. Data were apodized with an unshifted Gaussian in the direct dimension and with a sine-bell-square function (75˚-shifted) in both the ^{13}C and ^{15}N dimensions.

In the case of apoMb$_{119}$ in the presence of DnaK-β, known resonance assignments were used (3).

Resonances with extremely poor signal-to-noise or significantly overlapping with other resonances in 2D ^{1}H,^{15}N heteronuclear correlation spectra were discarded and not included in the analysis.

SUPPLEMENTARY TEXT

Native Gel Analysis of apoMb$_{119}$. Non-denaturing gels were run on a continuous McLellan buffer system at pH 5.8 similar to the one reported earlier (4). Briefly, the gels were run with a vertical electrophoresis apparatus (Bio-Rad, Hercules, CA) at constant voltage (200V) for 35 min at 4°C. Native gel analysis of the apoMb$_{119}$ soluble aggregate is shown in Figure S1 (left lane). As discussed in the main manuscript, it appears that a major species is present, though there may be some conformational heterogeneity with this species.

Native Gel Analysis of apoMb$_{119}$ in the presence of DnaK-β. In the presence of stoichiometric amounts of DnaK-β, the system shifts to a different distribution of states (Fig. S1, central lane). This result qualitatively illustrates the fact that addition of the chaperone has an effect on the soluble self-associated chaperone-free ensemble. The above gel data are consistent with previous studies on this system involving native gels and excision of the native gel bands followed by SDS gels and MALDI-TOF analysis (4). These investigations revealed that the broadly distributed bands found in the chaperone-apoMb$_{119}$ mixtures contain both chaperone and substrate (4). This result, in conjunction with the ligand-binding

NMR titration data of Figure 6c, suggests that the native gel bands for the 1:1 apoMb$_{119}$-DnaK-β mixture include some molecular complexes between apoMb$_{119}$ and DnaK-β. The multiple bands in the apoMb$_{119}$-DnaK-β mixture point to some heterogeneity. Given that the ligand-binding titrations show only moderate chemical shifts variations and no leveling-off is achieved, the chaperone is likely only loosely associated with the substrate and it interacts with the NMR-invisible N-terminal portion of the chain. Finally, it is worth noticing that the overall intensity of the gel band for the apoMb$_{119}$+DnaK-β sample is higher than expected, i.e., lower than the sum of the gel intensities for the apoMb$_{119}$-only and DnaK-β-only samples. This result suggests that some population of the soluble apoMb$_{119}$-only sample may be a very large aggregate unable to run through the gel. Such population would likely be NMR-undetectable, consistent with the model for the effect of the DnaK-β chaperone on the soluble apoMb$_{119}$ aggregate discussed below.

DnaK-β Structure. The three-dimensional structure of the substrate-binding domain of the DnaK chaperone, DnaK-β, determined by X-ray crystallography, is shown in Figure S2. DnaK-β is a single-domain predominantly β sheet protein and its binding site for substrates resides in a relatively narrow pocket close to the surface of the protein.

Overall NMR Features of apoMb$_{119}$ in the Presence of DnaK-β. The ^{1}H,^{15}N-HSQC spectrum of a 1:1 mixture of ^{15}N-labeled apoMb119 and unlabeled DnaK-β is shown in Figure S3. Only a fraction of the expected resonances is detectable, at the low temperature (4˚C) required to prevent macroscopic substrate aggregation. As in the case of the chaperone-free species, all of the detectable resonances correspond to the C-terminal portion of apoMb$_{119}$. The narrow chemical shift dispersion of the backbone amide protons indicates that the detectable segment of chaperone-associated apoMb$_{119}$ (i.e., the second half of the sequence) is highly disordered. The ^{1}H,^{15}N-HSQC NMR resonances of apoMb$_{119}$ in the presence of stoichiometric amounts of DnaK-β (Fig. S3) are virtually superimposable to those of chaperone-free apoMb$_{119}$ (Fig. 2). Therefore, the local environment of the C-terminal detectable resonances of the chaperone-bound substrate does not change significantly, upon addition of chaperone to the system. A significant number of resonances remain undetectable in both chaperone-free apoMb$_{119}$ and the apoMb$_{119}$-DnaK-β mixture due to either slow local tumbling or chemical exchange (see also section below on translational diffusion), or a mixture of the two. Therefore, we postulate that any interactions of apoMb$_{199}$ with DnaK-β take place in the NMR-undetectable N-terminal region of apoMb$_{199}$.

Backbone Dynamics of apoMb$_{119}$ in the Presence of DnaK-β. NMR relaxation experiments were performed on apoMb$_{119}$ in the presence of stoichiometric amounts of DnaK-β, to gain information about the nature of the complex. The results are shown in Figure S4. Steady-state ^{1}H-^{15}N NOE of apoMb$_{119}$ in the presence of DnaK-β were collected but are not presented here (see below). Although reduced spectral density functions could not be calculated for apoMb$_{119}$ in the presence of DnaK-β, they are not expected to differ significantly from those of apoMb$_{119}$, due to the similarity between R_1 and R_2. Overall, the R_1 and R_2 data are quite similar to those for chaperone-free apoMb$_{119}$. The R_1 rates are not much sequence-dependent, and the ^{15}N R_2 rates of apoMb$_{119}$ in complex with the chaperone gradually decrease from residues 65 to 95, and then again from 110 to 119 (Fig. S4).

Upon considering these results and the data in Figure 7 of the main text, reporting on the resonance intensity variations upon addition of the chaperones, we propose the following

model, for the interaction of $apoMb_{199}$ with the DnaK-β chaperone. First, the increase in NMR intensity is due to an enhancement in the spectroscopically detectable population of $apoMb_{119}$ resonances. The increased R_2s at the C-terminal edge, observed when the chaperone is added to the medium (Fig. S5), mainly reflect the fact that the soluble aggregate, whose formation is promoted by the chaperone, has a slightly larger average size in the presence of chaperone. The R_2s of the very flexible C terminal residues are particularly affected by interaction with the chaperone. We propose that the increase in size within the ensemble is due to the loose association of the DnaK-β chaperone to the N terminal region, consistent with the native gel results. The translational diffusion data presented in the next section provide additional support for this hypothesis.

NMR Translational Diffusion Experiments in the Presence of DnaK-β: Data Collection and Analysis. Diffusion coefficients were determined via the BPPSTE-HSQC pulse sequence (5). No ^{15}N chemical shift evolution was performed, to yield a 1-D version of the original pulse sequence. Gradient amplitudes were calibrated at 4°C according to published methods (6), using the known diffusion coefficient of $apoMb_{119}$ at pH 2.5 (4). The diffusion delay was set to 253 ms. The diffusion-encoding gradients (g_0) ranged from 0 to 60 G cm^{-1}.

Data processing was performed by the VNMR software (Varian) on a Sun workstation. No window functions were applied to the time-domain data. Diffusion coefficients were measured from the slope of $\ln(I/I_0)$ *vs* g_0^2 plots as described (4,5). I and I_0 denote resonance intensities (or integrals) at general g_0 values and $g_0=0$, respectively. Experimental values for I and I_0 were determined by peak integration. A baseline correction was applied to all spectra prior to integration by fitting the experimental baseline to a seventh order polynomial.

NMR Diffusion Experiments in the Presence of DnaK-β. The NMR diffusion experiments on $apoMb_{119}$ in the presence of DnaK-β performed in this work yielded a diffusion constant of 2.68 x 10^{-11} m^2s^{-1}. This value is slightly smaller than that of chaperone-free $apoMb_{119}$, indicating an even slower translational diffusion for the DnaK-β-$apoMb_{119}$ complex. This result is consistent with the idea that chaperone bound $apoMb_{119}$ forms a larger complex than chaperone-free $apoMb_{119}$ (see description of the proposed model for the soluble aggregate in the presence of the DnaK-β chaperone in the previous section). Although chaperone binding at equilibrium may be only partial, the average effect of chaperone binding is sensed by the increase in diffusion coefficient.

The translational diffusion coefficient, D, of a spherical/elliptical shaped molecule is

$$D = \frac{k_B T}{6\pi\eta R_H F} \quad , \qquad (7)$$

where k_B is the Boltzmann constant, T is the temperature, η is the viscosity and F is Perrin shape factor, whose value depends on particle shape. F is > 1 for an ellipsoid and equal to 1 for a sphere. Relation 7 shows that changes in both molecular shape and size can affect on translational diffusion. The potential effect of molecular shape is briefly discussed below.

Elongated particles experience greater frictional forces than spheres of equivalent volume, and consequently undergo slower diffusion. Modeling an $apoMb_{119}$: DnaK-β complex as a prolate ellipsoid in the limiting case with the long axis corresponding to the fully extended $apoMb_{119}$ chain and short axis the width of the chain with and without including DnaK-β, yields a Perrin factor of 5.26 and 2.13, respectively. The calculated value for the Perrin factor using the above diffusion coefficient is 2.34. Since the experimentally observed D value falls between the limiting cases of a sphere and a rigid prolate ellipsoid of

revolution considered above, the observed D may reflect the presence of some spherical or partially elongated apoMb$_{119}$:DnaK-β complexes in the ensemble.

NMR Sample Preparation. NMR samples of apoMb$_{119}$ in the presence of the DnaK-β chaperone were prepared as follows. Concentrated stock solutions of ^{15}N-labeled apoMb$_{119}$ at pH 2.5 were diluted to 100 μM in 20mM sodium acetate and 5mM KCl containing 5% D_2O. DnaK-β (100 μM total concentration) was then added, and the solution pH was adjusted to 6.0 with 0.1M KOH. The low protein and chaperone concentrations ensured that DnaK-β, which is not a highly soluble species, did not undergo any undesired aggregation in solution before the addition of substrate. After mixing all components, the solution pH was adjusted to 6.0. All NMR samples were equilibrated overnight at 4°C prior to data acquisition.

NMR Spectroscopy in the Presence of DnaK-β: General Procedures for Data Collection and Processing. NMR data collection was carried out as described in the main manuscript except for the fact that spectral widths in the ^{1}H and ^{15}N dimensions, respectively, were set to 6,600 and 1,500 Hz, and relaxation delays were set to 1.5 s. The NMRPipe (7) and NMRView (8) software packages were used for data processing. The known resonance assignments of apoMb$_{119}$ in the presence of DnaK-β (3) were used. However, resonances with extremely poor signal-to-noise or significantly overlapping with other resonances in 2D ^{1}H,^{15}N heteronuclear correlation spectra were discarded and not included in the analysis. Resonance intensity assessments were based on previously collected (4) sensitivity-enhanced ^{1}H,^{15}N-CPMG-HSQC (9) intensity distribution data reported on unassigned resonances. Here, the intensity of the subset of assigned (and well resolved in ^{1}H,^{15}N-CPMG-HSQC spectra) amide proton backbone resonances are reported, as a function of residue number. Due to the very low concentrations demanded by the scarce solubility of both apoMb$_{119}$ and DnaK-β, TROSY-type experiments (10-14) were not performed. Based on our prior experience on similar (non-^{2}H-enriched) systems, the expected gain in spectral resolution would likely not outbalance the signal loss resulting from multiplet component selection.

NMR Relaxation Measurements: Data Collection and Processing. ^{15}N T_1 and T_2 relaxation data were collected by procedures identical to those described in the main manuscript. In the case of this apoMb$_{119}$-DnaK-β sample, the poor signal-to-noise resulting from the low concentration prevented the collection of multiple T_1 and T_2 data sets for apoMb$_{119}$. Steady-state NOE data for this sample were collected but, due to the poor signal-to-noise, the results are not reported here.

REFERENCES

1. Fedyukina, D., S. Rajagopalan, A. Sekhar, E. C. Fulmer, Y.-J. Eun, and S. Cavagnero. 2010. Contribution of long-range interactions to the secondary structure of an unfolded globin. Biophysical Journal 99:L37-L39.
2. Kay, L. E., M. Ikura, R. Tschudin, and A. Bax. 1990. 3-Dimensional Triple-Resonance Nmr-Spectroscopy of Isotopically Enriched Proteins. Journal of Magnetic Resonance 89:496-514.

3. Chen, Z., N. Kurt, S. Rajagopalan, and S. Cavagnero. 2006. Secondary structure mapping of DnaK-bound protein fragments: chain helicity and local helix unwinding at the binding site. Biochemistry 45:12325-12333.
4. Kurt, N., S. Rajagopalan, and S. Cavagnero. 2006. Effect of Hsp70 chaperone on the folding and misfolding of polypeptides modeling an elongating protein chain. J. Mol. Biol. 355:809-820.
5. Rajagopalan, S., Chow, C., Raghunathan, V., Fry, C. G., Cavagnero, S. 2004. NMR spectroscopic filtration of polypeptides and proteins in complex mixtures. J. Biomol. NMR 29:505-516.
6. Antalek, B. 2002. Using pulsed gradient spin echo NMR for chemical mixture analysis: how to obtain optimum results. Conc. Magn. Reson. 14:225-258.
7. Delaglio, F., S. Grzesiek, G. W. Vuister, G. Zhu, J. Pfeifer, and A. Bax. 1995. NMRPipe - a multidimensional spectral processing system based on Unix pipes. J. Biomol. NMR 6:277-293.
8. Johnson, B. A. and R. A. Blevins. 1994. NMRView - a computer program for the visualization and analysis of NMR data. J. Biomol. NMR 4:603-614.
9. Mulder, F. A. A., C. Spronk, M. Slijper, R. Kaptein, and R. Boelens. 1996. Improved HSQC experiments for the observation of exchange broadened signals. Journal of Biomolecular Nmr 8:223-228.
10. Pervushin, K., R. Riek, G. Wider, and K. Wuthrich. 1997. Attenuated T-2 relaxation by mutual cancellation of dipole-dipole coupling and chemical shift anisotropy indicates an avenue to NMR structures of very large biological macromolecules in solution. Proceedings of the National Academy of Sciences of the United States of America 94:12366-12371.
11. Tzakos, A. G., C. R. R. Grace, P. J. Lukavsky, and R. Riek. 2006. NMR techniques for very large proteins and RNAs in solution. Annual Review of Biophysics and Biomolecular Structure 35:319-342.
12. Wider, G. and K. Wuthrich. 1999. NMR spectroscopy of large molecules and multimolecular assemblies in solution. Current Opinion in Structural Biology 9:594-601.
13. Wider, G. 2005. NMR techniques used with very large biological macromolecules in solution. In Nuclear Magnetic Resonance of Biological Macromolecules, Part C. 382-398.
14. Fernandez, C. and G. Wider. 2003. TROSY in NMR studies of the structure and function of large biological macromolecules. Current Opinion in Structural Biology 13:570-580.
15. Stevens, S. Y., S. Cai, M. Pellecchia, and E. R. Zuiderweg. 2003. The solution structure of the bacterial HSP70 chaperone protein domain DnaK(393-507) in complex with the peptide NRLLLTG. Protein Sci. 12:2588-2596.
16. DeLano, W. L. 2002. The PyMOL User's Manual. Palo Alto, CA, USA: DeLano Scientific.

FIGURE LEGENDS

Figure S1. Native gel analysis of apoMb$_{119}$ and DnaK-β at pH 6.0. From left to right, the lanes illustrate the data for apoMb$_{119}$, apoMb$_{119}$ in complex with DnaK-β, and pure DnaK-β.

Figure S2. Three-dimensional structure of DnaK-β. Atomic coordinates were derived from PDB file 1Q5L, corresponding to a previously determined high resolution NMR structure of DnaK-β in complex with a small peptide (15). The image was created with the PyMOL software (16). The substrate binding site is denoted by an arrow.

Figure S3. ^{1}H,^{15}N-HSQC spectrum of ^{15}N,^{13}C-labeled apoMb$_{119}$ (100 μM) in the presence of stoichiometric amounts of unlabeled DnaK-β, in 20mM sodium acetate, 5mM KCl and 5% D_2O, at pH 6.0. The known spectral assignments (3) are indicated on the side of the respective resonances. In addition, the S58 and H64 resonances were also assigned but are not labeled on the spectrum due to their low intensity.

Figure S4. ^{15}N (a) R_1 and (b) R_2 relaxation rates of apoMb$_{119}$ in the presence of DnaK-β at pH 6.0 and 4 °C. The shaded area denotes the sequence chain regions corresponding to the assigned backbone residues. The black bars indicate the position of the native α-helices in full-length apomyoglobin.

Figure S5. Percent changes in ^{15}N (a) R_1 and (b) R_2 relaxation rates for apoMb$_{119}$ ^{1}H,^{15}N-HSQC upon addition of stoichiometric amounts of DnaK-β, plotted as a function of residue number. The shaded areas denote the sequence regions corresponding to the assigned backbone residues. The black bars above the plot indicate the sequence regions corresponding to the native α-helices of full-length apomyoglobin.

SUPPLEMENTARY FIGURES

Figure S1

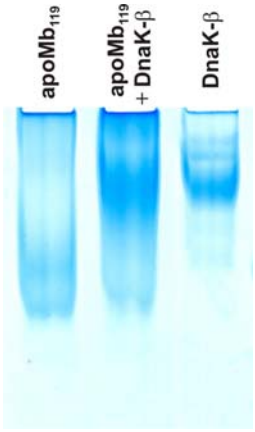

Figure S2

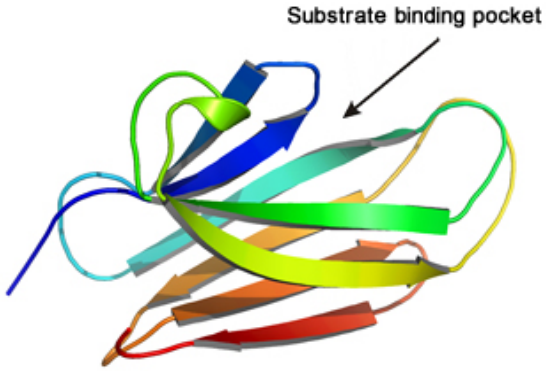

Figure S3

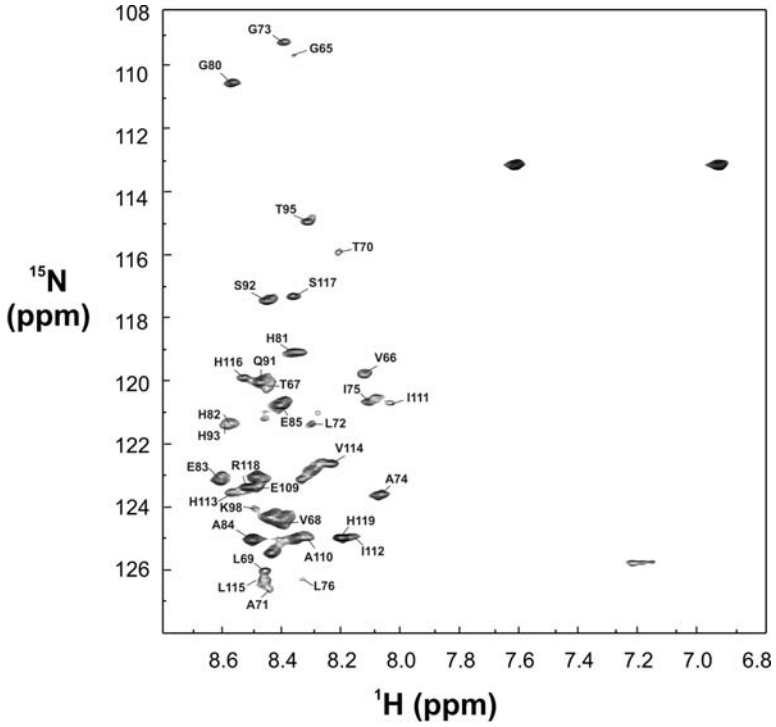
108
110
112
114
116
118
120
122
124
126
^{15}N (ppm)
8.6
8.4
8.2
8.0
7.8
7.6
7.4
7.2
7.0
6.8
^{1}H (ppm)
G73
G65
G80
T95
T70
S92
S117
H81
H116
Q91
V66
T67
I75
I111
H82
E85
L72
H93
V114
E83
R118
A74
E109
H113
K98
V68
H119
A84
I112
A110
L69
L115
L76
A71

Figure S4

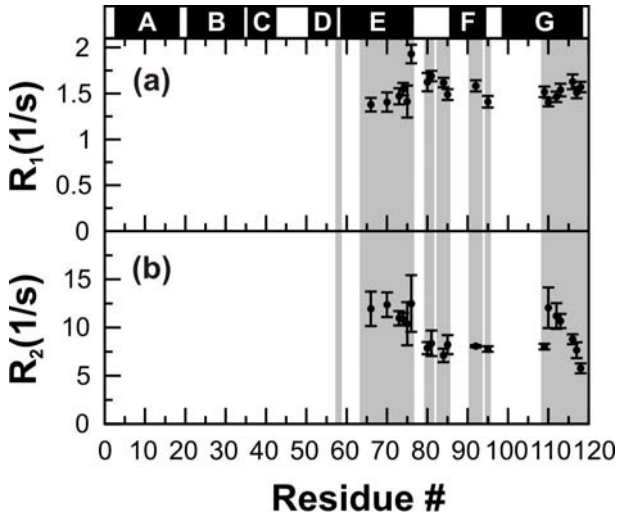
A
B
C
D
E
F
G
(a)
(b)
R_1(1/s)
R_2(1/s)
0
0.5
1
1.5
2
5
10
15
0 10 20 30 40 50 60 70 80 90 100 110 120
Residue #

Figure S5

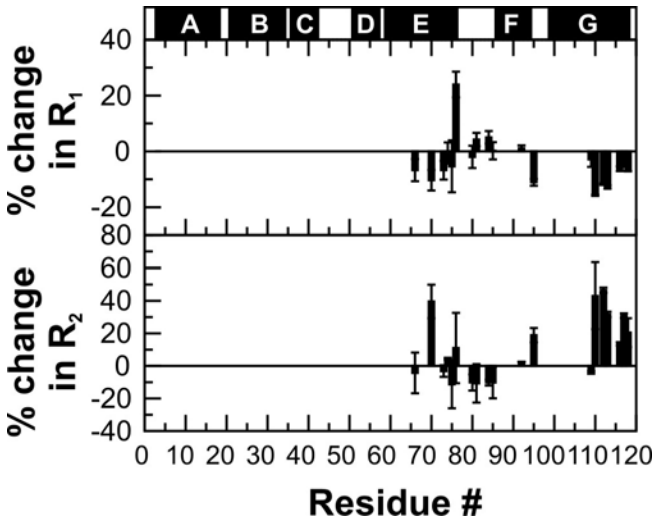
A
B
C
D
E
F
G
% change in R_1
% change in R_2
40
20
0
-20
80
60
40
20
0
-20
-40
0 10 20 30 40 50 60 70 80 90 100 110 120
Residue #